

A Rechargeable Li–O₂ Battery Using a Lithium Nitrate/*N,N*-Dimethylacetamide Electrolyte

Wesley Walker,* Vincent Giordani, Jasim Uddin, Vyacheslav S. Bryantsev, Gregory V. Chase, and Dan Addison

Liox Power, Inc., 129 North Hill Avenue, Suite 103, Pasadena, California 91106, United States

S Supporting Information

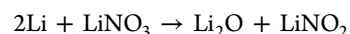
ABSTRACT: A major challenge in the development of rechargeable Li–O₂ batteries is the identification of electrolyte materials that are stable in the operating environment of the O₂ electrode. Straight-chain alkyl amides are one of the few classes of polar, aprotic solvents that resist chemical degradation in the O₂ electrode, but these solvents do not form a stable solid-electrolyte interphase (SEI) on the Li anode. The lack of a persistent SEI leads to rapid and sustained solvent decomposition in the presence of Li metal. In this work, we demonstrate for the first time successful cycling of a Li anode in the presence of the solvent, *N,N*-dimethylacetamide (DMA), by employing a salt, lithium nitrate (LiNO₃), that stabilizes the SEI. A Li–O₂ cell containing this electrolyte composition is shown to cycle for more than 2000 h (>80 cycles) at a current density of 0.1 mA/cm² with a consistent charging profile, good capacity retention, and O₂ detected as the primary gaseous product formed during charging. The discovery of an electrolyte system that is compatible with both electrodes in a Li–O₂ cell may eliminate the need for protecting the anode with a ceramic membrane.

Demand for better electric vehicles motivates the search for lower cost, higher capacity, rechargeable batteries. Aprotic electrolyte Li–O₂ batteries have received considerable attention due to very high theoretical specific energy, but degradation during cycling of every major component of the O₂ electrode, including solvent, lithium salt, binder and carbon, has plagued efforts to develop this technology for practical purposes.^{1–7} Recognition that the most successful Li-ion battery materials are unsuitable for use in Li–O₂ batteries has grown apace. In particular, solvents such as carbonates, ethers, esters, and lactones decompose in the presence of reactive oxygen species formed in the O₂ electrode.

Recently, the superior stability of *N,N*-dimethylformamide (DMF)⁸ and *N,N*-dimethylacetamide (DMA)⁹ in the O₂ electrode has been demonstrated by electrochemical mass spectrometry. In both cases, LiFePO₄ was used as a counter electrode in order to enable investigation of the O₂ electrode while avoiding problems caused by interaction of the solvent with a Li anode. The effective utilization of straight-chain alkyl amides as electrolyte solvents in Li–O₂ batteries has heretofore been limited due to interfacial instability with Li anodes. The present study demonstrates the successful operation of a

rechargeable Li–O₂ battery using a Li metal anode and an electrolyte consisting of DMA and lithium nitrate (LiNO₃). A cell with this electrolyte composition is shown to sustain reversible cycling for over 2000 h (>80 cycles) at a rate of 0.1 mA/cm², retaining >95% capacity and a consistent charging profile. Evidence for reversible formation and decomposition of Li₂O₂ is provided by XRD and *in situ* gas analysis.

Unprecedented electrolyte stability toward both the O₂ electrode and Li anode is achieved by combining a solvent having an amide core, which has been shown by quantum chemical calculations to be inert toward O₂ reduction products,⁹ with the nitrate anion, which is capable of forming a protective solid-electrolyte interphase (SEI) on Li. The reduction of the nitrate anion on Li metal was suggested¹⁰ to occur according to the following mechanism:



Previously, the incorporation of LiNO₃ into the electrolyte of Li–sulfur batteries was shown to improve cycling characteristics.^{11–13} LiNO₃ is thought to generate an SEI that effectively blocks the transfer of electrons from the Li anode to soluble, long-chain polysulfides that are released into the electrolyte during operation of the sulfur cathode. Consistent with these results, we find that LiNO₃ has a dramatic effect on stabilization of the Li/electrolyte interface in DMA.

A Li–O₂ cell consisting of a carbon paper cathode, a Li anode and an electrolyte of DMA and lithium bis-(trifluoromethanesulfonyl)imide (LiTFSI) shows massive overcharging (Figure 1, inset) starting at ~3.4 V vs Li/Li⁺, although electrochemical oxidation of this electrolyte begins at ~4.3 V on glassy carbon (Figure S1, Supporting Information [SI]). To better understand this phenomenon and to demonstrate the effect of LiNO₃, linear sweep voltammetry (LSV) was performed on two cells containing an untreated Li anode and a carbon paper cathode (Figure 1). The first cell, containing 1 M LiTFSI and no LiNO₃, shows multiple oxidation processes as the scan is performed from the open circuit potential to 4.3 V. These electrochemical processes are not observed in a cell containing 1 M LiNO₃ instead of LiTFSI. Our results show that the reaction between Li and DMA generates soluble species that are electroactive above 3.4 V and that inclusion of LiNO₃ in the electrolyte substantially inhibits the production of these electroactive species. Two small oxidation processes (<20 μA/cm² peak currents) are observed in the LiNO₃/DMA

Received: November 24, 2012

Published: January 29, 2013

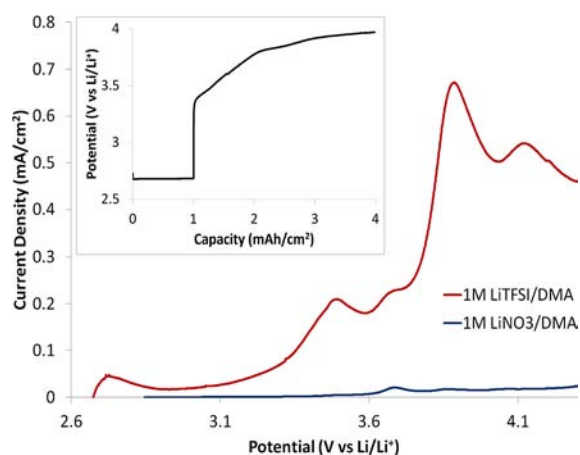


Figure 1. Linear sweep voltammograms on carbon paper electrodes (scan rate = 0.05 mV/s, 1 atm O₂, room temperature, OCV: 10 min.). (Inset) Galvanostatic cycling at 0.1 mA/cm² of a Li–O₂ cell in 0.5 M LiTFSI/DMA at 30 °C.

electrolyte at ~3.7 and 3.9 V, which may correspond to the oxidation of dissolved nitrite anions, consistent with the proposed reaction between LiNO₃ and Li metal.¹⁰

In a second experiment, the stability of the 1 M LiNO₃/DMA electrolyte toward Li metal was further tested using a three-electrode cell consisting of a Super P carbon (Csp) cathode, a Li disk anode, and a Li reference electrode (Figure 2). Cycling this cell at 0.1 mA/cm² demonstrated low

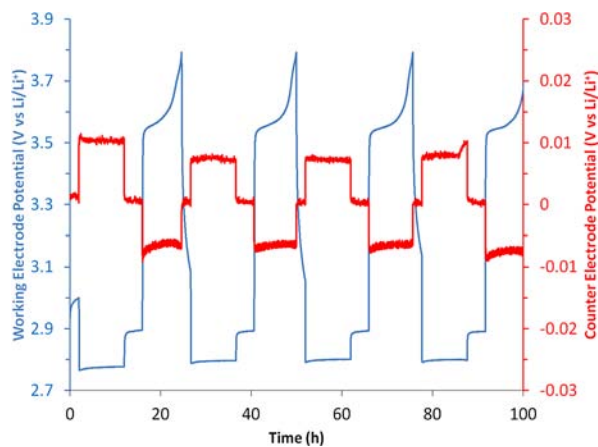


Figure 2. Three-electrode cell galvanostatic cycling utilizing a Csp cathode, a Li anode, a lithium reference electrode, and 1 M LiNO₃/DMA electrolyte. The cell was cycled under 1 atm O₂ at a rate of 0.1 mA/cm², with a dwell at OCV between each half cycle. Discharge was limited to 1 mA·h/cm², and charge was limited to 3.8 V. Room temperature.

overpotentials (~10 mV) for plating and stripping Li in the LiNO₃/DMA electrolyte with little drift in the voltage profile. Additionally, the OCV remained constant after each half cycle. The consistency of the charge/discharge plateaus in Figure 2 of the Li electrode demonstrates that the interfacial resistance at the Li metal surface changes negligibly. This behavior provides evidence for the stability of the SEI formed in the presence of LiNO₃ and consequent inhibition of the reaction between DMA and Li. Further indication for this inhibition can be found in the voltage profile of the O₂ electrode. In contrast to the cell containing a LiTFSI/DMA electrolyte, no overcharging is

observed, with clear electrode polarization marking the end of the charging process. The elimination of overcharge in the LiNO₃/DMA cell is consistent with the disappearance of large oxidative peaks in the LSV experiment, observed when switching from LiTFSI to LiNO₃.

Li–O₂ cells containing 150 μL of 1 M LiNO₃/DMA electrolyte (Figures 3–5) were constructed and cycled at 0.1

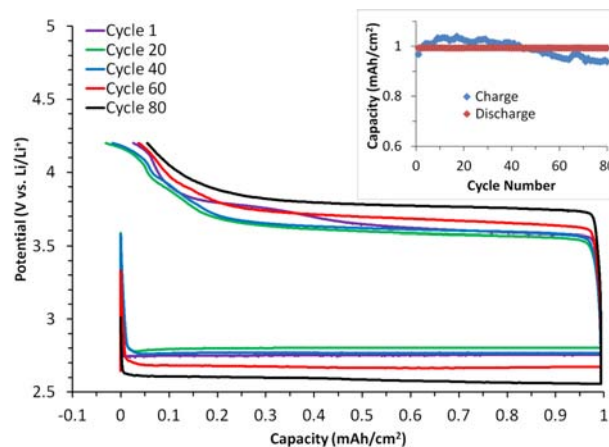


Figure 3. Voltage profiles for cycles 1, 20, 40, 60, and 80 of a Li/1 M LiNO₃ DMA (150 μL)/Csp cell cycled at 0.1 mA/cm² at room temperature (discharge limited to 10 h, charge limited to 4.2 V). (Inset) Plot of charge/discharge capacity by cycle number.

mA/cm². Details about testing fixtures and cell construction can be found in the SI. Lithium anodes were pretreated in a 1 M solution of LiNO₃/DMA in order to ensure the formation of a stable SEI prior to cell operation and to minimize the amount of LiNO₂ initially present in the cell. It was found that a concentration of 1 M LiNO₃ was required in cells to eliminate signs of reaction between DMA and the Li anode.

Over 2000 h (80+ cycles) of cycling was achieved when discharge was capacity limited to 1 mA·h/cm² (~220 mA·h/g of Csp) and charge was voltage limited to 4.2 V. Although high cycle numbers have been achieved in Li–O₂ cells using carbonate- and ether-based electrolyte systems, the observation that CO₂ is the main gaseous product evolved during charging indicates that electrolyte decomposition occurs rapidly in these cells.^{1,2} In order to evaluate the stability of the DMA/LiNO₃ electrolyte system, *in situ* mass spectrometry was performed to identify the gases evolved during cycling. O₂ is the primary gas detected for each charge half cycle throughout all 2000 h of operation (with comparatively small CO₂ and H₂ signals discussed below), indicating that electrochemical oxidation of Li₂O₂ is the primary electrode process taking place during charging (Figure 4). In each charge half cycle, ~1 mA·h of charge is passed (±5%) before the cell polarizes to 4.2 V. During the last 5% of the charge half cycles, O₂ evolution decreases, and CO₂ evolution occurs as the cell begins to polarize, suggesting that side reactions have not been completely eliminated. Previous research indicates that reaction between carbon and O₂ reduction products leads to the formation of small amounts of Li₂CO₃. The problem of carbon stability lies beyond the scope of the present study. Carbon decomposition may account for the differences in discharge and charge capacity and the onset of CO₂ evolution at the end of charge, but the possibility that relatively slow side reactions involving the electrolyte are taking place cannot be completely

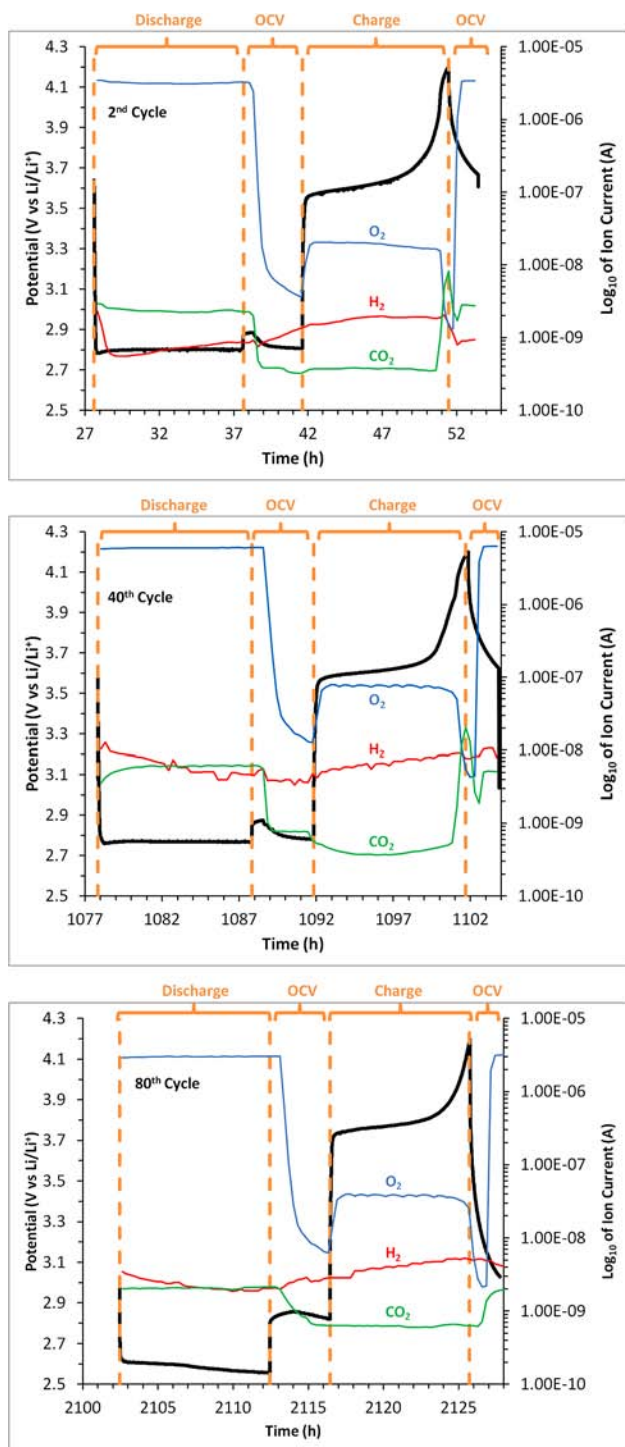


Figure 4. Gas profiles of cycles 2, 40, and 80 of a Li/1 M LiNO₃ DMA (150 μL)/Csp cell, room temperature, cycled at 0.1 mA/cm². During each cycle the cell was discharged for 10 h under O₂, followed by a 4 h OCV dwell to switch the gas environment from O₂ to Ar, followed by a charge to 4.2 V under Ar, and finally a 2 h OCV to switch from an Ar to O₂ environment.

discounted. Avoidance of problems associated with carbon instability was a motivation for employing a shallow cycling protocol. Cells that were deep discharged to 2.5 V have a capacity of ~2200 mA·h/g of carbon on the first discharge with O₂ remaining the main gaseous product formed during

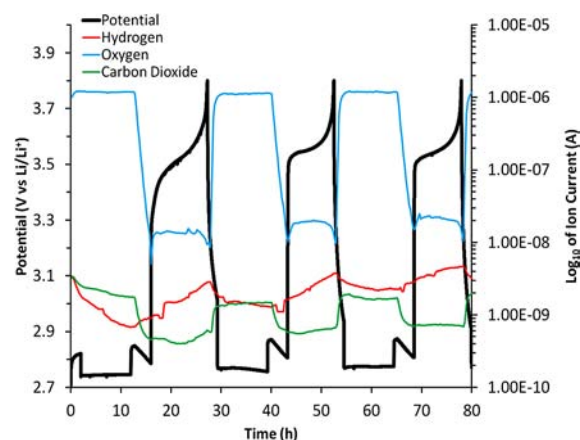


Figure 5. Gas profile of a Li/1 M LiNO₃ DMA (150 μL)/Csp cell cycled at 0.1 mA/cm² at room temperature. During each cycle the cell was discharged 10 h under O₂, followed by a 4 h OCV to swap gases from O₂ to Ar, followed by a charge to 3.8 V under Ar, and finally a 2 h OCV to switch from Ar to O₂ environment.

charging, but capacity fades rapidly, with 65% capacity retention after 5 cycles (Figure S3, SI).

For the first ~1000 h of cell operation, the charge and discharge profiles remain mostly unchanged in terms of shape, potential and capacity. The only exception is found in the first cycle where an extra peak around 3.7–3.8 V is observed, which is believed to result from LiNO₂ oxidation. It is speculated that LiNO₂ forms initially because manipulation of the lithium disk from the pretreatment solution exposes fresh Li surface to dissolved LiNO₃. As cycling is continued past ~1000 h, an increase in polarization during both discharge and charge and capacity loss during charge is noted. One cause for performance loss in the present study is solvent evaporation. Electrodes and separators harvested from cells following long-term cycling appeared to be substantially dry. Solvent evaporation could not be completely eliminated in the present study as gas sampling for mass spectrometry required cell gas volumes to be purged periodically.

Discharge of the cells was performed under 1 atm O₂. No significant H₂ or CO₂ was observed during discharge in all cycles. Every discharge was followed by a dwell at OCV for 4 h in order to switch the gas environment from O₂ to Ar, thus enabling the detection of O₂ evolution during charging. It is important to note that during the OCV period following discharge, the baseline level of CO₂ decreases. This change is likely due to oxidation of carbon impurities in the filament of the mass spectrometer when O₂ is used as a carrier gas and not from processes occurring in the cell. In each cycle, a small amount of H₂ is generated during the charge half cycle. The source of the H₂ signal is unknown, but a possible source is the reaction of a small amount of DMA with the Li anode as new Li metal surface is exposed. Finally, CO₂ gas is detected as polarization occurs at the end of charge in each cycle for the first ~1600 h of the experiment, indicating either oxidation of the solvent or oxidation of a side product formed from carbon corrosion during cycling (Figure 4, cycles 2 and 40). The presence of CO₂ is consistent with the slight overcharge observed in cell operation for the first ~1000 h. However, for cycles above ~1600 h, there is no evolution of CO₂ gas at the end of charge (Figure 4, cycle 80). Furthermore, polarization at the end of charge becomes visibly sharper.

Additionally, it is notable that when the charging potential is limited to 3.8 V, no CO₂ signal is detected during polarization at the end of charge (Figure 5). Observed CO₂ may originate from the oxidation of decomposition products of either carbon or the electrolyte (e.g., Li₂CO₃) formed during cycling. It is doubtful that the CO₂ signal is caused by direct electrochemical oxidation of the solvent (see electrochemical stability window, Figure S1, SI), but the possibility that Li₂O₂ catalyzes electrochemical oxidation of the solvent cannot be completely precluded.

XRD analysis was performed in order to identify the products formed during discharge of the cell (Figure 6).

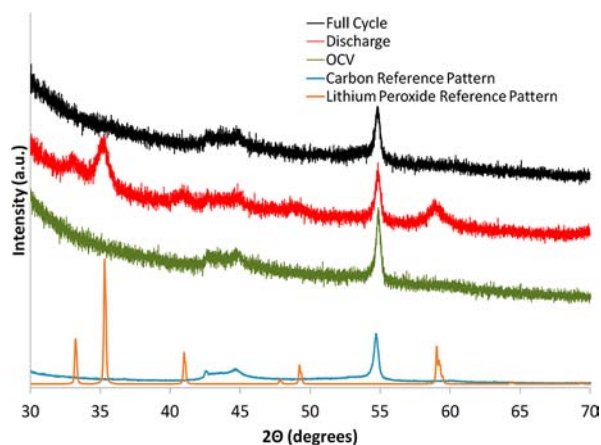


Figure 6. XRD analysis of a control electrode, a discharged electrode and a cycled electrode along with reference diffraction patterns for carbon and Li₂O₂.

Three cells were constructed in Swagelok-type fixtures using a 7 mg carbon paper cathode and 1 M LiNO₃/DMA electrolyte. Carbon paper electrodes were chosen for this experiment because the lower surface area compared to that of Csp yields clearer XRD signals, although replicate experiments on Csp demonstrated similar qualitative results. The first cell was constructed and maintained at OCV under O₂ for 100 h and operated as a control for the experiment. The second cell was discharged to 2 V at a rate of 0.1 mA/cm², resulting in ~5 mA·h/cm² discharge capacity. The third cell was discharged at the same rate and then recharged to 4.1 V at the same rate resulting in ~100% Coulombic efficiency. The resulting XRD analysis performed under Kapton tape confirms that the control only shows reflections associated with carbon. The discharged cell shows reflections at 33°, 35°, 41°, 48°, 49°, 59° 2θ which is consistent with the formation of Li₂O₂. Finally the fully cycled cell does not reveal diffraction patterns for Li₂O₂. Altogether, XRD analysis confirms within the detection capabilities of the instrument that Li₂O₂ is formed during discharge and consumed during charge. However, it is possible that small amounts of products are present but exist in amounts that are below the detection limit of the instrument or are amorphous. Furthermore, the presence of Li₂O₂ has been confirmed after 10 cycles in a cell containing a DMA electrolyte via XRD.⁹

In conclusion, this work has demonstrated for the first time the operation of a Li–O₂ battery with a Li anode using a straight-chain alkyl amide electrolyte solvent. A Li–O₂ cell utilizing a 1 M LiNO₃/DMA electrolyte is able to undergo shallow cycling at 0.1 mA/cm² for over 2000 h. Cells exhibit good capacity retention and minimal evolution of CO₂ and H₂

gases upon charging to 4.2 V vs Li/Li⁺. Furthermore, it has been demonstrated that CO₂ evolution can be eliminated by limiting charges to 3.8 V. Future work needs to be undertaken to more fully understand the nature of the SEI and to quantitatively assess the relationship between charge passed and the consumption and evolution of O₂. However, the electrolyte composition described in this work demonstrates unprecedented stability toward both the O₂ electrode and Li anode. The stability of this system can be attributed to the inertness of the amide core toward reactive oxygen species combined with the ability of the nitrate anion to contribute to the formation of a protective SEI that inhibits reaction between the solvent and the Li anode. Heretofore it has been assumed that a ceramic membrane separating the anode and cathode compartments is required in order to enable the use of solvents that are unstable toward Li metal yet advantageous regarding the O₂ electrode. The use of an SEI-forming Li salt instead of a ceramic membrane to prevent reactivity with the Li anode provides a new direction for Li–O₂ battery research and creates opportunities in the identification of stable combinations of cell components.

■ ASSOCIATED CONTENT

📄 Supporting Information

Materials and methods, the electrochemical stability window of the LiTFSI/DMA electrolyte on glassy carbon, ¹H NMR spectra of the LiNO₃/DMA electrolyte before and after prolonged cycling in a Li–O₂ cell, and the voltage profile of a Li–O₂ cell cycled in LiNO₃/DMA electrolyte without discharge capacity restriction. This material is available free of charge via the Internet at <http://pubs.acs.org>.

■ AUTHOR INFORMATION

Corresponding Author

wes@lix.com

Notes

The authors declare no competing financial interest.

■ REFERENCES

- (1) Freunberger, S.; Chen, C.; Peng, Z.; Griffin, J.; Hardwick, L.; Bardé, B.; Novák, P.; Bruce, P. *J. Am. Chem. Soc.* **2011**, *133*, 8040.
- (2) Freunberger, S.; Chen, Y.; Drewett, N.; Hardwick, L.; Bardé, F.; Bruce, P. *Angew. Chem., Int. Ed.* **2011**, *50*, 8609.
- (3) Bryantsev, V.; Giordani, V.; Walker, W.; Blanco, M.; Zecevic, S.; Uddin, J.; Addison, D.; Chase, G. *J. Phys. Chem. A* **2011**, *115*, 12399.
- (4) McCloskey, B.; Bethune, D.; Shelby, R.; Grishkumar, G.; Luntz, A. *J. Phys. Chem. Lett.* **2011**, *2*, 1161.
- (5) Veith, G.; Nanda, J.; Delmau, L.; Dudney, N. *J. Phys. Chem. Lett.* **2012**, *3*, 1242.
- (6) Black, R.; Oh, S.; Lee, J.; Yim, T.; Adams, B.; Nazar, L. *J. Am. Chem. Soc.* **2012**, *134*, 2902.
- (7) McCloskey, B.; Speidel, A.; Scheffler, R.; Miller, D.; Viswanathan, V.; Hummelshøj, J.; Nørskov, J.; Luntz, A. *J. Phys. Chem. Lett.* **2012**, *3*, 997.
- (8) Chen, Y.; Freunberger, S.; Peng, Z.; Barde, F.; Bruce, P. *J. Am. Chem. Soc.* **2012**, *134*, 7952.
- (9) Bryantsev, V.; Uddin, J.; Giordani, V.; Walker, W.; Addison, D.; Chase, G. *J. Electrochem. Soc.* **2013**, *160*, A160.
- (10) Poris, J.; Raistrick, I.; Huggins, R. *Proc. Electrochem. Soc.* **1984**, *84-2*, 313.
- (11) Mikhaylik, Y. U.S. Patent, 7,352,680, 2008.
- (12) Aurbach, D.; Pollak, E.; Elazari, R.; Salitra, G.; Kelley, C.; Affinito, J. *J. Electrochem. Soc.* **2009**, *156*, A694.
- (13) Liang, X.; Wen, Z.; Liu, Y.; Wu, M.; Jin, J.; Zhang, H.; Wu, X. *J. Power Sources* **2011**, *196*, 9839.